J Solid State Electrochem (2006) 10: 575–580
DOI 10.1007/s10008-006-0144-9

ORIGINAL PAPER

David S. Mebane · Meilin Liu

Classical, phenomenological analysis of the kinetics of reactions at the gas-exposed surface of mixed ionic electronic conductors

Received: 23 December 2005 / Accepted: 15 January 2006 / Published online: 13 April 2006

Abstract The kinetics of reactions occurring at the gas-exposed surfaces of charged mixed ionic electronic conductors (MIECs) are examined from theoretical first principles. Analysis based on the classical electrochemical potential-transition state theory model reveals that the nature of the reactions is electrochemical in general. However, the influence of the surface potential on the reaction rate is opposite for adsorption and incorporation reactions. Two-dimensional finite volume models of an MIEC as working electrode in a half-cell configuration are presented. The results for a simple, two-step reduction process show that the effect of the surface potential on the rate of reactions is minimal for incorporation-limited reactions but more influential for adsorption-limited reactions.

Keywords Adsorption · Electrode reaction kinetics · Perovskite-type crystals · Electric current–potential relationship · Fuel cell cathodes

Introduction

One of the most interesting and dynamic areas of study in the field of mixed ionic electronic conductors (MIECs) involves the phenomenological picture of reactions occurring on the gas-exposed surface of a charged MIEC. These reactions appear to be chemical rather than electrochemical reactions in a traditional, familiar sense: no net current flows across the electrified interface at a steady state. Yet some elementary steps of the reactions at the gas–MIEC interface do involve the transfer of electrons between the bulk MIEC and some adsorbed surface species (see Fig. 1). The question then becomes as follows: Are the rates of these reactions directly or indirectly controlled by the outside potential applied to the MIEC?

The question has divided solid state electrochemists. Many argued that these air surface reactions were purely chemical (as opposed to electrochemical), primarily because the reactions occurring at gas-exposed surfaces do not involve a net transfer of current across the boundary [1–4]. Others maintained that the rates of reactions at the surface may be influenced directly by the surface potential, in a manner concordant with the Butler–Volmer equation [5, 6].

The work of Vayenas and co-workers on the response of Pt surface species to applied potential forces a refinement of the question. The work of Vayenas et al. focuses on the electrochemical promotion of Pt-catalyzed oxidation reactions. A wealth of experimental data produced in the course of studying this phenomenon indicates that the application of outside potential to a Pt working electrode on a solid electrolyte influences the surface potential through adsorbates on the Pt surface. This, in turn, influences the rate of chemical reactions occurring on the surface (see [7] and citations therein). However, as Fleig and Jamnik point out in a theoretical analysis inspired by Vayenas et al.'s work, the influence of applied potential on the surface potential is not necessarily a direct proportionality [8].

In a subsequent paper, Fleig analyzed the gas-surface kinetics problem for MIECs [9]. The analysis was notable for its use of electrochemical rate expressions to describe surface processes. However, the Butler–Volmer style expressions for adsorption and incorporation Fleig started with respond in a direct manner to polarization changes at the MIEC–gas interface, as opposed to the overpotential applied to the MIEC. Similar to the results for Pt, the analysis for MIECs reveals a complex relationship between the overpotential applied at the electrode and the reaction rate. This work is a significant step forward in our theoretical understanding of gas-surface reactions on MIECs.

This work will complement Fleig's in two respects. First, we provide a derivation of the relevant phenomenological rate expressions from first principles. Second, we incorpo-

D. S. Mebane · M. Liu (✉)
School of Materials Science and Engineering,
Georgia Institute of Technology,
Atlanta, GA 30332-0245, USA
e-mail: meilin.liu@mse.gatech.edu
Tel.: +1-404-8946114
Fax: +1-404-8949140

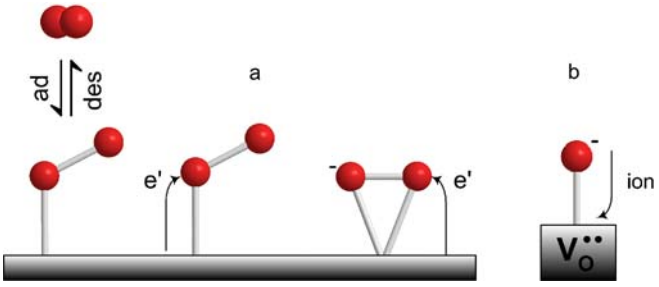

Fig. 1 (**a**) Electron transfer from MIEC to the LUMO of oxygen to form O_2^- and O_2^{2-} (**b**) oxygen ions combine with vacancies on the surface of the MIEC. Although each step represents a reaction involving charge transfer, the overall reaction results in zero net charge transferred out of the MIEC

rate these expressions into a phenomenological model of an MIEC cathode and use the results to draw conclusions affecting the debate on whether the reactions occurring at the surface can be described by purely chemical rate expressions.

Analysis

The following analysis will follow the electrochemical potential-transition state theory derivation first published by Parsons [10], but also appearing in Erdey-Gruz [11], Delahay [12], and Bockris et al. [13]. The analysis contains several assumptions, although these assumptions do not prevent general conclusions from being drawn on the kinetic phenomenology at MIEC–gas interfaces. The discussion following the analysis presents a pair of examples that, while not universally relevant, nonetheless illustrate some important implications.

Consider the reaction at the oxygen-exposed surface of an MIEC electrode conducting oxygen vacancies and electron holes under cathodic polarization:

$$\frac{1}{2}O_2 + V_{O,MIEC}^{\bullet\bullet} \rightarrow O_{O,MIEC}^{x} + 2h_{MIEC}^{\bullet} \tag{1}$$

Now consider a simple breakdown of reaction 1 into dissociative adsorption and incorporation steps:

$$\frac{1}{2}O_2 + s \rightarrow O_{ads}^{-} + h^{\bullet} \tag{2}$$

$$O_{ads}^{-} + V_O^{\bullet\bullet} \rightarrow O_O^x + h + s \tag{3}$$

where s represents an adsorption site on the surface of the MIEC. Figure 2 depicts the standard free energy surface along a reaction coordinate for a reaction under cathodic polarization. Analyzing reaction 2, the standard free energies for states I and II are:

$$\overline{\mu}_{I,2}^0 = \frac{1}{2}\mu_{O_2}^0 \tag{4}$$

$$\overline{\mu}_{II,2}^0 = \mu_{O^-}^0 - F\varphi_s + \mu_h^0 + F\varphi_m \tag{5}$$

where φ is the electrostatic potential, and the subscripts m and s refer to the MIEC just beneath the surface and on the surface, respectively. The key to the derivation is the introduction of the transfer coefficient, α, which allows for the definition of the electrical part of the free energy in the activated state:

$$\overline{\mu}_{A,e}^0 - \overline{\mu}_{I,e}^0 = \alpha\left(\overline{\mu}_{II,e}^0 - \overline{\mu}_{I,e}^0\right) \tag{6}$$

where the subscript e refers to the electrical part of the electrochemical potential. Equation 6 leads to an expression for the standard free energy of the activated state:

$$\overline{\mu}_{A,2}^0 = \mu_{A,2}^0 + \alpha_2 F(\varphi_m - \varphi_s) \tag{7}$$

According to transition state theory, the rate constant of any elementary reaction is given by:

$$k = \kappa\frac{k_B T}{h_p}\exp\left(\frac{-\Delta G_A^0}{RT}\right) \tag{8}$$

where κ is the transmission coefficient, k_B is Boltzmann's constant, h_P is Planck's constant, and ΔG_A^0 is the standard activation energy. Equations 4, 5, 7 and 8 now yield expressions for the forward and backward rate constants in reaction 2:

$$\vec{k}_2 = \vec{\kappa}_2\frac{k_B T}{h_p}\exp\left[\frac{-\left(\mu_{A,2}^o - \mu_{O_2}^o + \alpha_2 F\chi\right)}{RT}\right] \tag{9}$$

$$\overleftarrow{k}_2 = \overleftarrow{\kappa}_2\frac{k_B T}{h_p}\exp\left[\frac{-\left(\mu_{A,2}^o - \mu_{O^-}^o - \mu_h^o + (\alpha_2 - 1)F\chi\right)}{RT}\right] \tag{10}$$

where $\chi = \varphi_m - \varphi_s$ is the surface potential. The forward and backward rates for the reaction are therefore:

$$\vec{r}_2 = \vec{k}_2'\exp\left[\frac{-(\alpha_2 F\chi)}{RT}\right]a_{O_2}^{1/2}a_s \tag{11}$$

$$\overleftarrow{r}_2 = \overleftarrow{k}_2'\exp\left[\frac{(1-\alpha_2)F\chi}{RT}\right]a_h a_{O^-} \tag{12}$$

where the k' terms are a set of collected constants, and a represents the activity. Assuming dilute concentrations of surface species and holes and ideal gas, the following expression emerges for the overall rate of reaction 2:

$$r_2 = \vec{k}_2'' \exp\left(\frac{-\alpha_2 F\chi}{RT}\right) P_{O_2}^{1/2} \Gamma(1-\theta) - \overleftarrow{k}'' \exp\left(\frac{(1-\alpha_2)F\chi}{RT}\right) c_h \Gamma\theta \tag{13}$$

where θ is the occupied site fraction, Γ is the total density of surface sites, and c_h is the concentration of holes at the MIEC surface. The k'' terms now include activity coefficients, assumed constant.

When reaction 2 is at equilibrium, r=0. The forward and backward terms are then both equal to a constant, which is the exchange rate:

$$k_2^0 = \vec{k}_2'' \exp\left(\frac{-\alpha_2 F\chi_0}{RT}\right) P_{O_2,0}^{1/2} \Gamma(1-\theta_0) = \overleftarrow{k}_2'' \exp\left(\frac{(1-\alpha_2)F\chi_0}{RT}\right) c_h \Gamma\theta_0 \tag{14}$$

where the subscript 0 denotes the equilibrium value. Factoring out k^0 from Eq. 13 yields the familiar form of the equation:

$$r_2 = k_2^0 \left[\frac{P_{O_2}^{1/2}(1-\theta)}{P_{O_2,0}^{1/2}(1-\theta_0)} \exp\left(\frac{-\alpha_2 F\Delta\chi}{RT}\right) - \frac{c_h\theta}{c_{h,0}\theta_0} \exp\left(\frac{(1-\alpha_2)F\Delta\chi}{RT}\right) \right] \tag{15}$$

where $\Delta\chi$=χ −χ_0.

Turning attention to reaction 3, the relevant standard electrochemical potentials are:

$$\overline{\mu}_{I,3}^0 = \mu_{O^-}^0 - F\varphi_s + \mu_V^0 + 2F\varphi_m \tag{16}$$

$$\overline{\mu}_{II,3}^0 = \mu_h^0 + F\varphi_m \tag{17}$$

$$\overline{\mu}_{A,3}^0 = \mu_{A,3}^0 + F(2\varphi_m - \varphi_s) + \alpha_3 F(\varphi_s - \varphi_m) \tag{18}$$

Taking these expressions through the same procedure as above, the forward and backward rate constants become:

$$\vec{k}_3 = \vec{k}_3 \frac{k_B T}{h_p} \exp\left[\frac{-\left(\mu_{A,3}^o - \mu_{O^-}^o - \mu_V^o + -\mu_V^0 - \alpha_3 F\chi\right)}{RT}\right] \tag{19}$$

$$\overleftarrow{k}_3 = \overleftarrow{k}_3 \frac{k_B T}{h_p} \exp\left[\frac{-\left(\mu_{A,3}^o - \mu_h^o - (\alpha_3 - 1)F\chi\right)}{RT}\right] \tag{20}$$

This leads to the expression for the rate of reaction 3:

$$r_3 = \vec{k}_3'' \exp\left(\frac{\alpha_3 F\chi}{RT}\right) c_\nu \Gamma\theta - \overleftarrow{k}_3'' \exp\left(\frac{-(1-\alpha_3)F\chi}{RT}\right) c_h \Gamma(1-\theta) \tag{21}$$

and the corresponding introduction of an exchange rate constant:

$$r_3 = k_3^0 \left[\frac{c_\nu\theta}{c_{\nu,0}\theta_0} \exp\left(\frac{\alpha_3 F\chi}{RT}\right) - \frac{c_h(1-\theta)}{c_{h,0}(1-\theta_0)} \exp\left(\frac{-(1-\alpha_3)F\chi}{RT}\right) \right] \tag{22}$$

Discussion

Assuming that both adsorption and incorporation are thermally activated, elementary steps, the results presented in Eqs. 15 and 22 show that the effects of the surface potential on the rates of adsorption and incorporation must be opposed. (That is, tending to increase the rate of one and to decrease the rate of the other.) The observation that r_2=r_3 at steady state leads to a significant implication of this: the

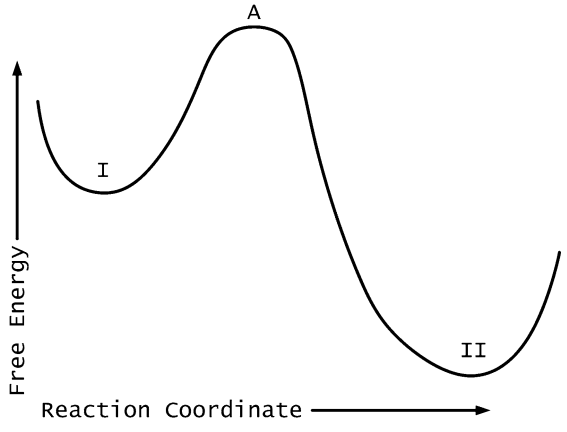

Fig. 2 Reduced dimensionality free energy surface for charge transfer reactions

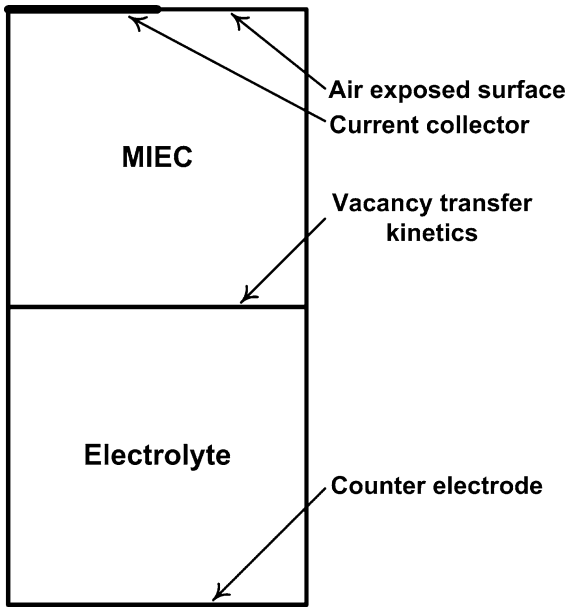

Fig. 3 Schematic of the model geometry for the MIEC half-cell model. The *vertical sides* on each side are considered to be symmetrical boundaries

chemical (preexponential) terms in Eqs. 15 and 22 must play a dominant role in one or both reactions.

To illustrate this point, a 2D model of a dense, patterned MIEC electrode in a half-cell experimental setup was created. The geometry of the test cell appears in Fig. 3. The model utilizes the reaction mechanisms 2, 3 and the attending rate expressions 15 and 22 as flux boundary conditions at the air surface of the MIEC. The other features of the model are dilute solution transport theory (with holes and vacancies as mobile defects), no surface diffusion, and electroneutrality. The surface potentials are calculated using a Helmholtz model of the double layer, which allows calculation of the potential difference from the site fraction of adsorbates. The method of solution is an iterative finite volume method. (The full derivation of the model will appear in a forthcoming paper.)

Table 1 lists values for parameters in the model. Most are adapted from approximate data given by Svensson et al. for perovskite MIECs $La_xSr_{1-x}(Co, Mn)O_{3\pm\delta}$ (LSC and LSM) [4, 14]. One exception is the equilibrium concentration of holes, which is loosely based on the defect chemistry of LSM, but chosen for the most part in order to create an MIEC rich in electronic species. The other exceptions are the exchange rate constants for adsorption and incorporation, which hew closely to Svensson et al.'s numbers for the first run but are modified for the second as described below. The model geometry is a 1-μm square, with a regular mesh size of 0.01-μm square for run 1 and 0.1-μm square for run 2. (Slower convergence times necessitated a coarser mesh for run 2.) Applied potential across the half cell is −0.1 V for both runs. All charge transfer coefficients are assumed to be 0.5.

For the first run of the model, the incorporation and adsorption exchange rate constants remain in the ranges given by Svensson et al., which is to say that the incorporation constant is much lower (by six orders of magnitude). The vacancy distribution in the MIEC is shown in Fig. 4. Note that the distribution is nearly uniform, with very gentle concentration gradients leading towards the air surface, but throughout the level, it is much higher than the equilibrium value for vacancies in the MIEC. The site fraction of adsorbates on the MIEC surface (not shown) is nearly uniform across the surface and is almost exactly equal to the equilibrium value of the adsorbate concentration. (The numbers are actually higher than the equilibrium value listed in Table 1 by much less than 1%.)

This result makes sense in consideration of the mechanisms 2 and 3. A high exchange rate constant for the adsorption reaction ensures that Eq. 2 stays very close to equilibrium, which means that the concentration of adsorbates and, correspondingly, surface potentials remain close to their equilibrium values. As a result, the potential dependent terms in Eq. 22 have almost no effect on the rate of incorporation. Instead, the increase in the concentration of vacancies in the MIEC drives the reaction.

The situation changes when the adsorption step becomes rate limiting. For the second run of the simulation, an

Table 1 Parameters used in the simulation

Parameter	Value, run 1	Value, run 2
$c_{v,0}$	2.0×10^{-4} mol/m^2	Same
$c_{h,0}$	300.0 mol/m^2	Same
Background charge in electrolyte	-6.4×10^{7} C/m^2	Same
Exchange rate constant for vacancy exchange at MIEC electrode boundary	3.0×10^{-2} mol/m·s	Same
k^0_{inc}	1.0×10^{-8} mol/m·s	1.0×10^{-2} mol/m·s
k^0_{ads}	1.0×10^{-2} mol/m·s	1.0×10^{-6} mol/m·s
θ_0	2.0×10^{-3}	Same
T	1,173 K	Same
Vacancy mobility in MIEC	1.0×10^{-12} mol·m^2/J·s	Same
Vacancy mobility in electrolyte	1.0×10^{-12} mol·m^2/J·s	Same
Hole mobility in MIEC	1.0×10^{-11} mol·m^2/J·s	Same
Γ	1.0×10^{-3} mol/m	Same

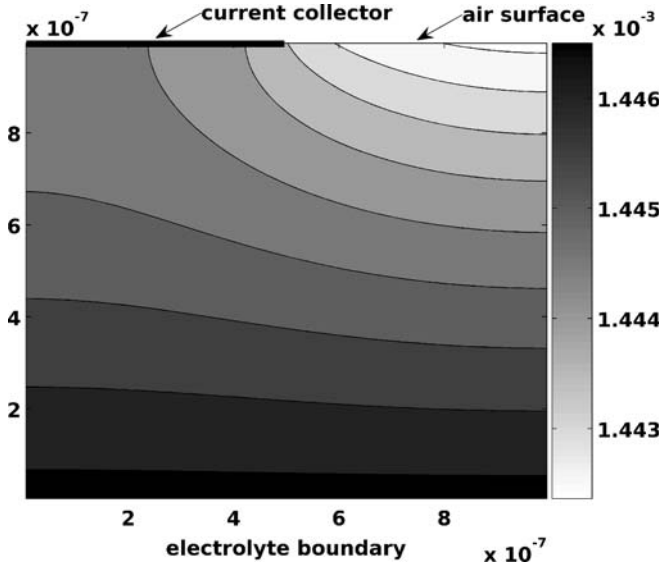

Fig. 4 Vacancy distribution in the MIEC, mol/m^2, for model run 1

adsorption rate constant of 10^{-6} mol/m·s and an incorporation constant of 10^{-2} mol/m·s were used. Figure 5 shows the vacancy distribution, which rises to a similar average value as that of the incorporation-limited case, although the gradient in concentration is slightly higher. However, the adsorbate site fraction in this case deviates significantly from equilibrium. The change is negative, with the concentration at steady state approximately 8% less than the equilibrium value on average. This tends to drive the adsorption reaction faster through both chemical and potential-dependent terms in Eq. 15. In effect, the surface potential changes in such a manner as to drive the slower adsorption reaction, whereas the faster incorporation reaction relies on the chemical driving force associated with the change in vacancies.

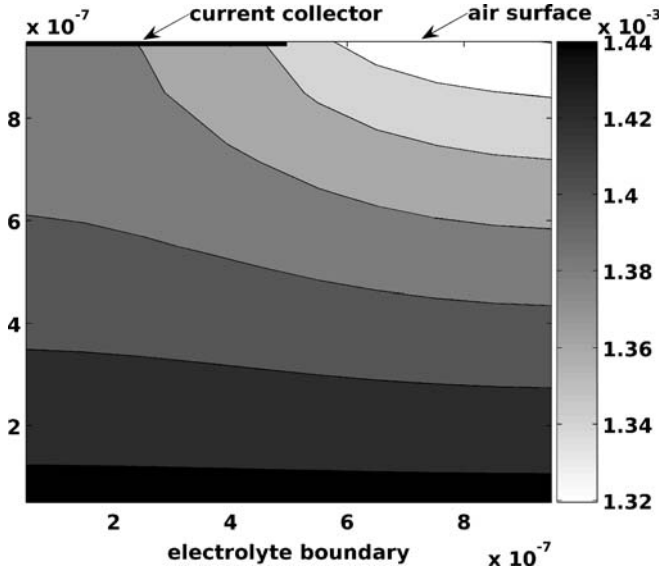

Fig. 5 Vacancy distribution in the MIEC, mol/m^2, for model run 2

Which scenario is more likely in reality? Equation 21 shows that the incorporation exchange rate constant, k_3^0, involves a product of the equilibrium concentration of vacancies and the equilibrium site fraction. In MIECs used in solid oxide fuel cells, such as LSM and LSC, both numbers are small. This suggests that incorporation exchange rate constants may be low on the surfaces of these materials. If that is the case, one expects that the concentrations of surface species *as a whole* on the MIEC surface will not deviate appreciably from equilibrium. This, of course, is the same situation one would expect if the rate expressions were affected by deviations of chemical concentrations from equilibrium only. The effect of the potential-dependent terms is, in general, simply to reinforce the chemical response of the rate of an elementary process to changes in adsorbate concentrations. For an adsorption-dominated mechanism, for instance, the deviation of adsorbate concentration from equilibrium is not as large as it would be in the case of purely chemical rate control.

For more complicated mechanisms involving more than one adsorbed species, the picture becomes more interesting. For example, a buildup of charged, chemisorbed peroxide moeties (O_2^{2-}) due to a slow dissociation step would have the effect of increasing the rate of the oxygen incorporation reaction.

Conclusion

Classical kinetic analysis for a simple breakdown of the reaction occurring at the gas-exposed surface on MIECs results in a set of equations that depend on changes in the surface potential in an exponential fashion, implying that the nature of the reactions is electrochemical in general. However, the effect of surface potential is opposite for adsorption and incorporation steps, requiring that chemical driving forces play a dominant role at some point in the course of the overall reaction. Whether the reaction is electrochemically or merely chemically controlled, therefore, depends on the specific mechanism and the identity of the rate limiting step(s). 2D simulations of MIECs in half-cell configurations show that, for a simple reaction mechanism involving dissociative adsorption and incorporation on the MIEC surface only, the change in surface potential is negligible for an incorporation-controlled mechanism but appreciably negative for an adsorption-controlled one.

Acknowledgements This work was supported by the U. S. Department of Energy, the National Energy Technology Laboratory, through the SECA Core Technology Program (Grant No. DE-FC26-02NT41572). Additional support for David Mebane is provided by The Boeing Company, through a Boeing Fellowship.

References

1. Adler SB, Lane JA, Steele BCH (1996) J Electrochem Soc 143:3554

2. Adler SB, Lane JA, Steele BCH (1997) J Electrochem Soc 144:1884
3. Coffey GW, Pederson LR, Rieke PC (2003) J Electrochem Soc 150:A1139
4. Svensson AM, Sunde S, Nisancioglu K (1997) J Electrochem Soc 144:2719
5. Liu ML, Winnick J (1999) Solid State Ionics 118:11
6. van Heuveln FH, Bouwmeester HJM (1997) J Electrochem Soc 144:134
7. Vayenas CG, Brosda S, Pliangos C (2003) J Catal 216:487
8. Fleig J, Jamnik J (2005) J Electrochem Soc 152:E138
9. Fleig J (2005) Phys Chem Chem Phys 7:2027
10. Parsons R (1951) Trans Faraday Soc 47:1332
11. Erdey-Gruz T (1972) Kinetics of electrode processes. Wiley-Interscience, Budapest
12. Delahay P (1965) Double layer and electrode kinetics. Interscience, New York
13. Bockris JOM, Reddy AKN, Gamboa-Aldeco M (1998) Modern electrochemistry 2A: fundamentals of electrodics. Kluwer/Plenum, New York
14. Svensson AM, Sunde S, Nisancioglu K (1998) J Electrochem Soc 145:1390